Analysis of an actively-cooled coaxial cavity in a 170GHz 2MW gyrotron using the multi-physics computational tool MUCCA

Analysis of an actively-cooled coaxial cavity in a 170GHz 2MW gyrotron using the multi-physics computational tool MUCCA / Bertinetti, A.; Albajar, F.; Avramidis, K. A.; Cau, F.; Cismondi, F.; Gantenbein, G.; Jelonnek, J.; Kalaria, P. C.; Ruess, S.; Rzesnicki, T.; Savoldi, L.; Zanino, R.. - In: FUSION ENGINEERING AND DESIGN. - ISSN 0920-3796. - ELETTRONICO. - 146(2019), pp. 74-77. [10.1016/j.fusengdes.2018.11.033]

Analysis of an actively-cooled coaxial cavity in a 170 GHz 2 MW gyrotron using the multi-physics computational tool MUCCA

A. Bertinetti[a], F. Albajar[b], K. A. Avramidis[c], F. Cau[b], F. Cismondi[d], G. Gantenbein[c], J. Jelonnek[c],
P. C. Kalaria[c], S. Ruess[c], T. Rzesnicki[c], L. Savoldi[a], R. Zanino[a]

[a]NEMO Group, Dipartimento Energia, Politecnico di Torino, Torino, Italy
[b]Fusion for Energy, Barcelona, Spain
[c]Institute for Pulsed Power and Microwave Technology, Karlsruhe Institute of Technology, Karlsruhe, Germany
[d]EUROfusion, Garching, Germany

Continuous Wave gyrotrons are the key elements for Electron Cyclotron Resonance Heating and Current Drive (ECRH&CD) in present fusion experiments and future fusion reactors. In the frame of the EUROfusion activities, a 170 GHz, 2 MW short-pulse (~ 1 ms), water-cooled coaxial gyrotron, already tested at Karlsruhe Institute of Technology (KIT), is being upgraded for operation at longer pulses (~ 100 - 1000 ms).

Here we use the MUlti-physiCs tool for the integrated simulation of the CAvity (MUCCA), recently developed in collaboration between Politecnico di Torino and KIT, to analyze the evolution of the operating condition of the coaxial gyrotron cavity, self-consistently coupling thermal-hydraulic, thermo-mechanical and electro-dynamic models. The main results are presented in terms of evolution of temperature, heat load and deformation of the heated surface of the resonator and of the coaxial insert during the first few seconds of operation. We show that the system evolves towards stable operating conditions (no beam loss), with a peak temperature strongly dependent on the cooling configuration, where a large room for the improvement of the current cavity cooling design is found.

Keywords: Electron Cyclotron Resonance Heating and Current Drive (ECRH&CD), Gyrotron, Coaxial cavity, Multi-physics, Simulation.

1. Introduction

In the EU-DEMO perspective, [1] high power coaxial-cavity gyrotrons for heating the plasma and for driving a non-inductive current into it are under development at the Karlsruhe Institute of Technology (KIT) within the framework of EUROfusion activities [2]. The aim is to extend the ~ 1 ms pulse length of the existing 170 GHz, 2 MW coaxial-cavity tube up to 1 s [3,4]. Fig. 1 shows the cross section of the bottom part of the 170 GHz, 2 MW gyrotron which is characterized by the presence, inside the ~ 150 mm long cavity, of the coaxial insert (~ 1200 mm long, in total). The high-frequency wave is generated inside the cavity by resonant interaction between the electron beam, produced by a Magnetron Injection Gun (MIG) at the lower part of the gyrotron, and the high-frequency electromagnetic field in the cavity [5].

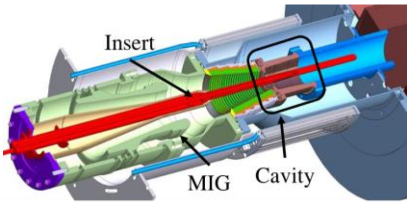

Fig. 1. CAD model of the coaxial cavity [2].

A very high ohmic heat-load results on the cavity and insert surfaces; therefore, both are subject to a deformation that modifies the resonating volume and changes the working condition of the gyrotron. A forced flow of pressurized subcooled water, passing around the resonator as well as through the insert by means of two independent cooling circuits, is used to maintain the cavity region as cold as possible to avoid damages ($T_{max} <$ 250 °C) and to reduce the thermal deformation of the surfaces.

2. Description of the coaxial cavity geometry

The cross section of the cavity and coaxial insert are shown in Fig. 2a, where the internal structure of the two components is also displayed.

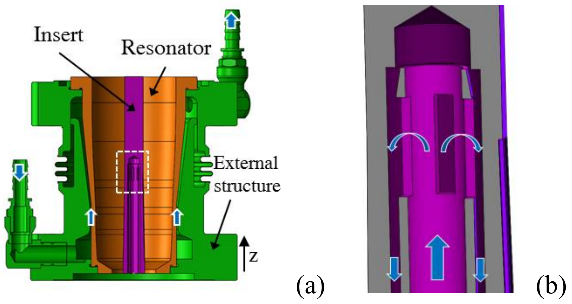

Fig. 2. Cross sections of the cavity (a) and the coaxial insert (b). Blue arrows indicate the main water flow directions.

The cavity is made of two different regions: the resonator and the external structure. The coolant flows in

---

author's email: laura.savoldi@polito.it

the annular region between the resonator and the external structure (see Fig. 2a, blue arrows) and exits from the outlet pipe on the top – inlet and outlet pipe are located on opposite parts of the cavity, inducing a non-fully uniform mass flow around the cavity. The part of the coaxial insert, which is simulated in this work is shown in purple in Fig.2a. The main coolant pathway in the top region of the coaxial insert is described by blue arrows in Fig. 2b. The water flows toward the upper region of the insert in the inner channel, then moves to the external region by means of four rectangular holes and finally flows toward the outlet in the external annular duct.

The resonator structure is made of Glidcop®, a copper-base alloy, the external structure of the cavity is made of stainless steel and the coaxial insert is made of copper.

3. Simulation strategy and setup

The MUlti-physiCs tool for the integrated simulation of the CAvity (MUCCA) has been developed in collaboration between Politecnico di Torino and KIT [6], [7]. MUCCA is applied here to the analysis of the cavity of the upgraded 170 GHz, 2 MW coaxial gyrotron to assess the evolution of its operating point, starting from cold conditions. A coupled procedure is adopted, where transient thermal-hydraulic (TH), followed by steady state thermo-mechanical (TM) simulations (the TM timescales are much faster than the TH ones) are first performed on the resonator and the insert with the commercial software STAR-CCM+ [8], evaluating the mechanical deformation of the surface of the two components. The deformed shapes are then used as input in the electro-dynamic (ED) code EURIDICE [9] to evaluate the heat loads on the walls, which become in turn the driver of the TH analysis in the following time step. The lack of symmetry on the geometry of the cavity cooling system does not allow a simplification of the resonator domain; on the contrary, ¼ of the domain of the coaxial insert is simulated.

Constant coolant mass flow rates of ~ 1 kg/s and 0.165 kg/s at constant temperature of 40 °C (corresponding to 130 ºC subcooling) are imposed at the inlet section of the cavity and of the coaxial insert, respectively. The pressure at the outlet section of the cavity and of the insert is set in order to measure an absolute pressure of 8 bar and 5.2 bar at the simulated inlet sections of the two components, respectively. The initial temperature of the solid structure is set everywhere equal to the inlet temperature of the coolant, assuming thermal equilibrium at the beginning of the transient.

The k-ω SST (Menter) turbulence model [10] with all-y+ wall treatment is adopted in the TH simulations, and the grid independence of the resulting temperature distribution of the heated surfaces has been checked. The average Reynolds numbers evaluate at the location of the heat load peak are ~15×10^3 and ~18×10^3 in the resonator and in the insert, respectively. The single-phase Rohsenow boiling model [11] implemented in STAR-CCM+ is used to evaluate the heat extracted by the coolant due to boiling, as in [12]. Fluid properties are set as a function of pressure and temperature (according IAPWS-IF97 library **Error! Reference source not found.**) and the copper **Error! Reference source not found.** and the Glidcop® [15] properties are a function of temperature.

The TM simulations are performed only on the resonator structure of the cavity and on the portion of the coaxial insert inside the cavity region. The top surface of the resonator and the bottom surface of the coaxial insert are fixed. "Normal constraints" impede the expansion of the lateral surface of the resonator, in order to simulate the contact with the external structure of the cavity, which is removed in the simulation. The other surfaces of the resonator region and of the coaxial insert are free to move. The reference temperature for the definition of the thermal unstressed condition of the solid structures is set to 27 °C. The deformation induced by the achievement of the thermal equilibrium of the solid structure with the coolant is also taken into account at the beginning of the transient; in particular, the shifting of the coaxial insert is evaluated considering also the axial thermal deformation of the lower part of the insert, which is not simulated here. The longitudinal expansion of the resonator induces the movement of the coaxial insert due to the mechanical connection between the two components in the region which is not taken into account in the simulation (see purple flange in Fig. 1). The heat load on the coaxial insert is shifted accordingly.

The deformed inner profile of the resonator and the deformed outer profile of the insert, which are computed by the TM module, are used in the ED simulation performed with the code EURIDICE for the evaluation of the interaction with the electron beam. The ED simulations consider operation at nominal parameters [4]. The updated temperature profiles from the TH simulations are also considered in the ED simulations to update the temperature dependent electrical conductivity of the surfaces.

The average heat load q due to ohmic heating on the resonating surface of the resonator and of the insert is computed by the standard formula

$$q = \frac{1}{2\sigma\delta}|\boldsymbol{H}_t|^2 \tag{1}$$

where $\boldsymbol{H}_t$ is the tangential component of the high frequency magnetic field, σ is the electrical conductivity of the surface, and δ is the skin depth.

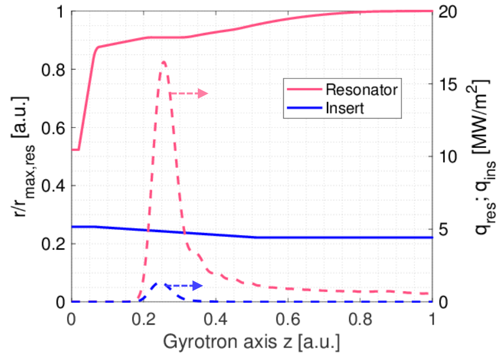

Fig. 3. Initial heat loads (dashed lines) and initial (non-deformed) heated surface radial profiles (solid lines) for the

resonator (red) and the insert (blue). The radial profile of the resonator and of the insert is scaled with the maximum radius of the resonator.

The initial heat load profiles applied on the resonator (q_{res}) and on the coaxial insert (q_{ins}) are shown in Fig. 3 together with the dimensionless radial profile of the heated surfaces of the two components. The co-rotating $TE_{34,19}$ mode (eigenvalue = 105.19) is selected as an operating mode. It is shown that q_{res} is ~ one order of magnitude higher than q_{ins}. The heat-load peaks, at the initial condition, are located approximately on the same axial position.

4. Results

The results of the application of MUCCA on the 170 GHz, 2 MW coaxial cavity are shown in terms of evolution of the hot spot temperature on the heated surface of the resonator and of the insert and of the peak heat loads (see Fig. 4).

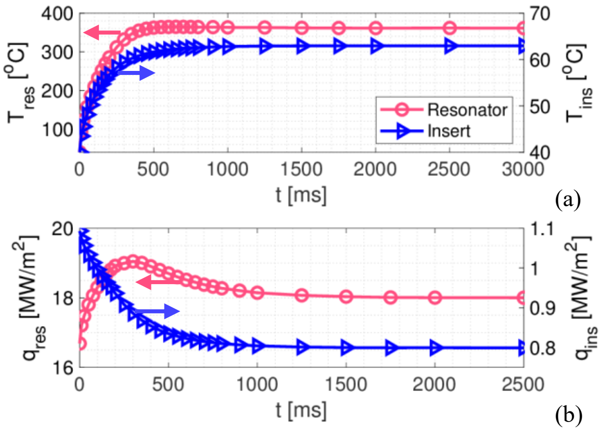

Fig. 4. Evolution of the maximum values for the resonator (open circles) and insert (open triangles) temperature (a) and heat load (b), respectively.

The peak temperatures and heat loads reach a steady state after ~ 1 s. Fig. 5 shows the evolution of the azimuthally averaged axial temperature profile of the resonator and of the coaxial insert heated surfaces (despite the azimuthal symmetry of the heat load on the cavity wall, averaging is needed because of the non-fully uniform flow distribution in the azimuthal direction, see above, leading to non-perfectly uniform temperature distribution). While the temperature peaks follow the behavior described in Fig. 4a, the temperature evolution on the upper part of the resonator (high z) and on the lower part of the insert (low z) is considerably slower, so that the steady state is not yet reached at t = 3 s. Boiling phenomena are observed in the resonator structure, localized in proximity of the heat load peak region. In the insert, while the heat load is symmetric, the temperature distribution in the axial direction shows some advection effects.

Fig. 4 and Fig. 5 show that, in order to keep the peak resonator surface temperature below 250 ºC, the pulse length should be kept below 150 ms. This is a very positive result with respect to the first phase of the upgrade of the coaxial gyrotron, which targets at ~100 ms pulse length. However, for the second phase of the upgrade, targeting at 1 s operation, the results suggest that an improvement of the resonator cooling is mandatory. According to the simulation results, no problems of overheating are visible on the co-axial insert, where the steady-state peak temperature is below 65 ºC.

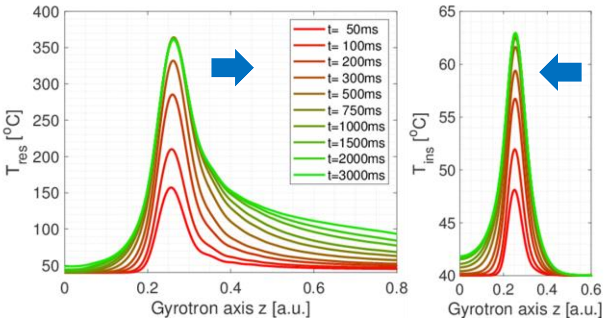

Fig. 5. Evolution of the average temperature along the heated surface of the resonator (left) and of the coaxial insert (right). Blue arrows indicate water flow directions.

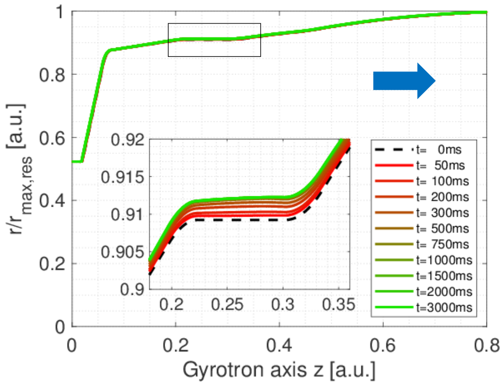

Fig. 6. Evolution of the radial profile of the heated surface of the resonator. The water flow direction is indicated by the blue arrow. The value of quality factor for the undeformed cavity (t = 0 ms) is 1677, which is decreased to 1283 for the deformed cavity (t = 3000 ms).

The evolution of the radial profile of the heated surface of the resonator is shown in Fig. 6. The relevant region for the cavity operation, where the beam-wave interaction primarily takes place, is highlighted in the inset. In the first part of the transient (t < 0.5 s) the radial profile of the resonator is subjected to a quick increase of radius caused by the evolution of the temperature peak. For t > 0.5 s, we compute a stabilization of the profile, which is characterized by a lower variation of the radial profile, driven by the temperature behavior of the downstream part of the resonator. The evolution of the radial profile in the coaxial insert is not reported here due to the very small deformation if compared to the resonator.

5. Preliminary results on alternative cavity cooling with mini-channels

Motivated by the overcoming, at time > 150 ms, of the limit temperature of 250 °C on the heated surface of the resonator with the annular cooling configuration, a preliminary steady state simulation is performed here, using the initial heat load on a different cooling layout. We consider a set of mini-channels (based on the idea presented in [6]) on the central section of the resonator (see Fig. 7).

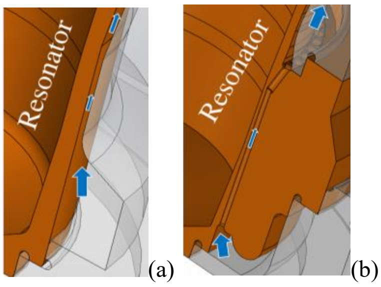

Fig. 7. CAD models of the annular (a) and of the mini-channels (b) cooling options of the coaxial cavity resonator. Blue arrows indicate the main water flow directions.

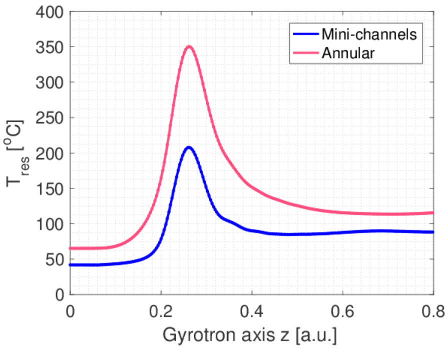

Fig. 8. Comparison of the steady state temperature profiles for alternative cooling configuration of the resonator.

The results are very promising: the modification induced by the use of the channels for the resonator cooling reduces the peak temperature by ~ 150 °C due to the more effective heat removal system (see Fig. 8). The temperature reduction in the mini-channels option is also due to the reduction of the thickness of the resonator with respect to the annular configuration. The new cavity design increases the coolant pressure drop from 0.6 bar (annular configuration) to 3.3 bar for the mini-channels configuration with the same mass flow rate, which remains acceptable for the operation of the gyrotron.

6. Conclusion

The MUCCA computational tool has been applied to analyze the current 170 GHz, 2 MW configuration of the coaxial gyrotron cavity developed at KIT. The evolution of the deformation of the inner surface of the resonator and of the external surface of the coaxial insert is simulated to assess the final operating condition of the gyrotron.

The simulation results show that the maximum temperature on the heated surface of the resonator region is kept below the acceptable limit of 250 °C for the first 150 ms of operation.

Preliminary simulation results on an alternative cooling strategy, where the resonator is equipped with a set of mini-channels for the coolant flow, show that this configuration could support even continuous-wave operation. This suggests that there is still large room for performance improvement, thanks to the possibility for a more accurate design of the cooling configuration of the resonator.

Acknowledgments

This work has been carried out within the framework of the EUROfusion Consortium and has received funding from the Euratom research and training programme 2014-2018 under grant agreement No. 633053. The views and opinions expressed herein do not necessarily reflect those of the European Commission. Part of the simulations was performed on the EUROfusion High Performance Computer (Marconi-Fusion).

References

[1] F. Romanelli et al., Fusion Electricity A roadmap to the realisation of fusion energy, EFDA, 2012.

[2] J. Jelonnek et al., Design considerations for future DEMO gyrotrons: A review on related gyrotron activities within EUROfusion, Fusion Engineering and Design 123 (2017) 241-246.

[3] T. Rzesnicki et al., Development and first operation of the 170 GHz, 2 MW longer-pulse coaxial-cavity modular gyrotron prototype at KIT, to appear at 43rd Int. Conf. on Infrared, Millimeter and THz Waves, 9 -14 September 2018, Nagoya, Japan.

[4] S. Ruess et al., KIT coaxial gyrotron development: From ITER towards DEMO, International Journal of Microwave and Wireless Technologies (2018) 1-9.

[5] M. V. Kartikeyan et al., Gyrotrons High-power Microwave and Millimeter Technology, Springer, 2004.

[6] A. Bertinetti et al., Multi-physics analysis of a 1 MW gyrotron cavity cooled by mini-channels, Fusion Engineering and Design 123 (2017) 313-316.

[7] K. A. Avramidis et al., Numerical studies on the influence of cavity thermal expansion on the performance of a high-power gyrotron, IEEE Trans. Electron Devices 65 (2018).

[8] Star-CCM+ User’s Manual v11.04.

[9] K. A. Avramides et al., EURIDICE: A code-package for gyrotron interaction simulations and cavity design, EPJ Web of Conferences 32 (2012).

[10] F. R. Menter, Review of the shear-stress transport turbulence model experience from an industrial perspective, International Journal of Computational Fluid Dynamics 23 (2009) 305-316.

[11] W. Rohsenow, A Method of Correlating Heat-Transfer Data for Surface Boiling of Liquids, Trans. of ASME, (1951) 969-976.

[12] A. Bertinetti et al., Design, Test and Analysis of a Gyrotron Cavity Mock-up cooled using Mini-Channels, IEEE Trans.

on Plasma Science 46 (2018) 2207-2215.

[13] http://www.iapws.org, January 2018.

[14] http://www-ferp.ucsd.edu/LIB/PROPS/PANOS/cu.html, January 2018.

[15] J.W. Davis, P.D. Smith, ITER material properties handbook, Journal of Nuclear Materials 233-237 (1996) 1593 -1596.